analytical chemistry

pubs.acs.org/ac Article

A Miniature Multilevel Structure for a Lossless Ion Manipulation Ion Mobility Spectrometer with Wide Mobility Range Separation Capabilities

Adam L. Hollerbach, Randolph V. Norheim, Pearl Kwantwi-Barima, Richard D. Smith, and Yehia M. Ibrahim*

Cite This: https://doi.org/10.1021/acs.analchem.1c04700 Read Online

ACCESS | Metrics & More | Article Recommendations | Supporting Information

ABSTRACT: Ion mobility spectrometry employing structures for lossless ion manipulations (SLIM-IMS) is an attractive gas-phase separation technique due to its ability to achieve unprecedented effective ion path lengths (>1 km) and IMS resolving powers in a small footprint. The emergence of multilevel SLIM technology, where ions are transferred between vertically stacked SLIM electrode surfaces, has subsequently allowed for ultralong single-pass path lengths (>40 m) to be achieved, enabling ultrahigh resolution IMS measurements to be performed over the entire mobility range in a single experiment. Here, we report on the development of a 1 m path length miniature SLIM module (miniSLIM) based on multilevel SLIM technology. Ion trajectory simulations were used to optimize SLIM board spacings and SLIM board thicknesses, and a new method of efficiently transferring ions between SLIM levels using asymmetric traveling waves (TWs) was demonstrated. We experimentally characterized the performance of the miniSLIM IMS-MS relative to a drift tube IMS-MS using Agilent tuning mixture cations and tetraalkylammonium cations. The miniSLIM achieved a resolving power of up to 131 (CCS/ΔCCS), which is ∼1.5× higher than achievable with a 78 cm path length drift tube IMS. Additionally, the entire ion mobility range was successfully transmitted in a single separation. We also demonstrated the miniSLIM's performance as a standalone IMS system (i.e., without MS), which showed baseline separation between all AgTM cations and a clear differentiation between different charge states of a standard peptide mixture. Overall, the miniSLIM provides a compact alternative to high performance IMS instruments possessing similar path lengths.

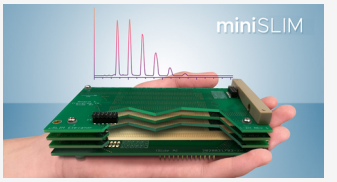

INTRODUCTION

Miniature ion mobility spectrometers (IMS) are highly attractive for their small size, light weight, and lower power consumption compared to their larger counterparts. The challenge when transitioning to a miniature IMS is maintaining sufficiently high separation power (i.e., resolving power and resolution).[1] Typically, IMS separation power can be enhanced by increasing (i) pressure, (ii) ion path length (absolute[2] and/or effective[3]), (iii) electric field strength, or some combination of the three.[4,5] High separation powers can also be achieved by trapping ions between a counteracting gas flow and voltage gradient and slowly decreasing the voltage gradient, as in trapped ion mobility spectrometry (TIMS),[6] or by using mixtures of buffer gases and/or slow changes in compensation voltage, as in field asymmetric waveform IMS (FAIMS).[7] While FAIMS and TIMS instruments can be quite small, they incur limitations due to ion transmission efficiency or space charge capacity. Voltage breakdown at or above certain pressures limits the maximum usable voltage, and a lack of effective confinement at elevated pressures limits the total usable path length (e.g., in drift tubes). The general miniaturization of IMS remains challenging, and a straightforward method for maintaining higher performance in conjunction with miniaturization is highly desirable.

Increasing IMS separation power (at low pressure) without changing instrument size is commonly performed by passing or cycling ions around the same ion path multiple times. Multipass methods provide increased effective path lengths (i.e., the path length ions actually travel), allowing higher resolving powers and resolutions to be achieved when many passes are used (via a $\sqrt{L}$ relationship, where L is the path length for one pass or cycle).[8−10] The main disadvantage of ion multipass methods is that faster ions eventually overtake (i.e., "lap") and pass slower ions if enough passes are allowed, resulting in convoluted mobility spectra. This means that multipass methods are best used to analyze a narrow ion mobility range in a single experiment, keeping in mind that ion mobility windows become narrower as the number of passes increases. Ion lapping issues are especially pronounced for cyclic miniature IMS systems, which normally employ short absolute path lengths.

Received: October 29, 2021
Accepted: December 8, 2021

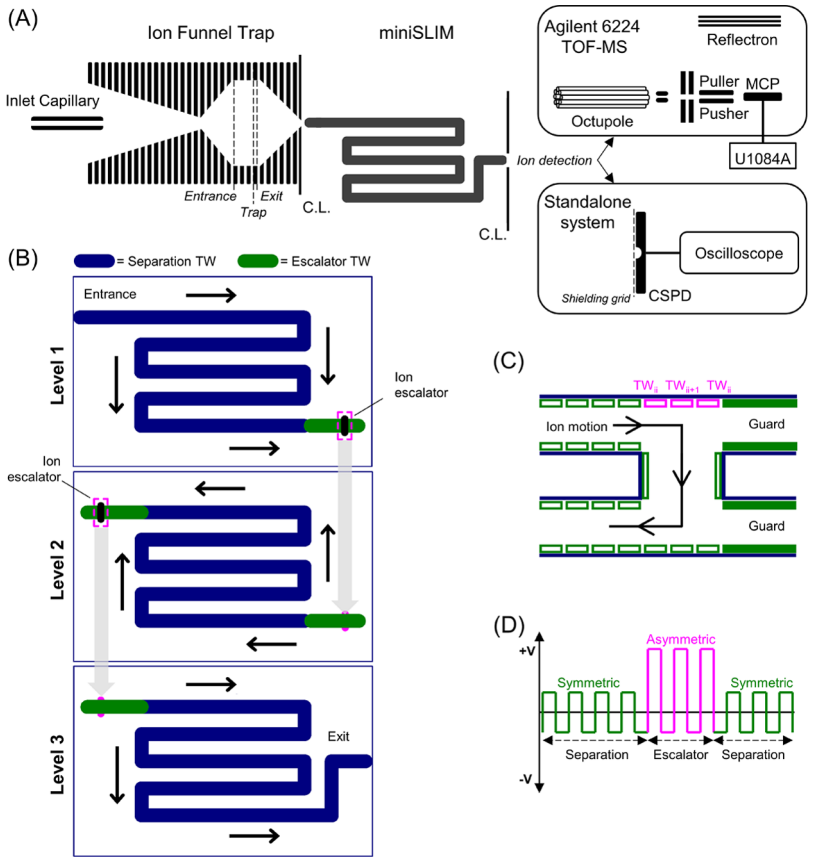

Figure 1. (A) Experimental schematic of the multilevel miniSLIM module and two ion detection methods. (B) Board layouts of all three miniSLIM levels. (C) Illustration of ion motion through an ion escalator employing asymmetric traveling waves. The leftmost and rightmost TW electrodes possess the same phase TW (ii), while the middle TW electrode possesses a 45° phase-shifted TW (ii + 1). (D) Depiction of symmetric and asymmetric traveling waves in the multilevel miniSLIM.

Long absolute path lengths have been established in IMS by using traveling wave (TW)-based IMS employing structures for lossless ion manipulations (SLIM-IMS).[11,12] In SLIM-IMS, TWs propel ions between two mirror-image surfaces possessing TW, RF, and DC guard electrodes. The electrodes can be arranged on printed circuit boards (PCBs) to create long serpentine path lengths (>10 m absolute path length) in a small footprint (e.g., 45.9 cm × 32.5 cm).[13] Additionally, ions that reach the end of the serpentine path can be sent back to the start of the SLIM path and allowed to pass through the serpentine path again to achieve truly unprecedented effective path lengths (e.g., >1 km).[14] However, issues associated with ion lapping remain even with such long absolute path lengths, and multiple separations are required to cover a broad mobility range.

To achieve ultrahigh resolution ion mobility separations without ion multipass methods, we developed a multilevel SLIM by vertically stacking dual-surface SLIM boards (i.e., PCBs with electrode arrays on each side).[15] Ions transfer between levels using "ion escalators" located at the ends of each ion track.[16] The long absolute path length (~43 m) achieved with a multilevel conventionally sized SLIM previously provided high resolution separations of phosphazene standards and complex mixtures of phosphopeptides over the entire mobility range of the sample.[15] Such ion escalator technology has provided substantial increases to the absolute path lengths already achievable in SLIM-IMS without changing the instrument footprint or using multipass methods, and a miniature version is a logical extension.

Here, we present the first miniature SLIM instrument (miniSLIM) using ion escalator technology to provide high resolution IMS separations over a wide mobility range without ion lapping. We used ion trajectory simulations to optimize and improve the performance of the ion escalators to ensure essentially lossless ion transmission using a new method for transferring ions between SLIM levels. The miniSLIM used three ion levels (33 cm path length per level), which established a total path length of 1 m. We characterized the performance of the optimized multilevel miniSLIM IMS when coupled to time-of-flight mass spectrometry (TOF-MS) using standard compounds and then as a fully functional standalone system. In all, the miniSLIM implementation provides a compact alternative to larger IMS instruments possessing similar path lengths.

EXPERIMENTAL SECTION

Chemicals and Electrospray Ionization. Tetraalkylammonium salts (TAA_C_2 – TAA_C_8) and solvents were purchased from Millipore-Sigma (St. Louis, MO, USA). Tetraalkylammonium salts (TAA_C_2 – TAA_C_8) were purchased as chloride, bromide, or hydrate salts and were diluted to a 1 μM equimolar mixture in acetonitrile. Nine peptide standards (angiotensin I, angiotensin II, bradykinin, fibrinopeptide A, kemptide, melittin, neurotensin, renin substrate tetradecapeptide, and substance P) were also

https://doi.org/10.1021/acs.analchem.1c04700
Anal. Chem. XXXX, XXX, XXX−XXX

purchased from Millipore-Sigma and diluted to a 10 μM equimolar mixture in 70:30 methanol:water. A low concentration Agilent tuning mixture was purchased from Agilent Technologies (Santa Clara, CA, USA) and used as received. Nanoelectrospray ionization (nESI) emitters (2−4 μm o.d.) were pulled from borosilicate glass capillaries (10 cm length, 1.5 mm o.d., 0.86 mm i.d.) using a P-2000 laser tip puller (Sutter Instruments, Novato, CA, USA). High voltage was applied to the solutions via a stainless-steel wire inserted into a microelectrode holder (Warner Instruments, Hamden, CT, USA).

Ion Optics and SLIM Instrumentation. The main components of the miniSLIM IMS module included a single inlet capillary (500 μm i.d.), an ion funnel trap (IFT),[17] and four vertically stacked PCBs comprising the miniSLIM (Figure 1A,B). When mass analysis was desired, ions were detected and digitized using an Agilent 6224-TOF-MS and U1084A 8-bit digitizer (Acqiris, Plan-les-Ouates, Switzerland) operating at 1 GS/s. When the miniSLIM was operated as a standalone system, an AcroMass charge-sensing particle detector (CSPD, Taipei, Taiwan) and Tektronix oscilloscope (DPO 5204B, Beaverton, OR, USA) were used. The TWs shown in the blue regions always possessed high speeds and low amplitudes for mobility separation, while the TWs shown in the green regions possessed either high or low speeds and amplitudes, depending on the experiment being performed. The pink regions indicate the locations of ion escalators.[15] Each ion level possessed ∼33 cm path length, yielding a total path length of ∼1 m for the miniSLIM. Board spacings and thicknesses were 2.80 and 1.65 mm, respectively. The dimensions of the assembled miniSLIM were 11.1 cm × 6.7 cm × 1.4 cm ($L \times W \times H$). Table S1 in the Supporting Information provides experimental dimensions for all electrode types used in the miniSLIM. Photographs of the assembled and disassembled miniSLIM are also provided in the Supporting Information (Figure S1).

Ion Escalator Using Asymmetric Traveling Waves. The miniSLIM utilized asymmetric TWs (i.e., TWs with higher amplitudes and a DC bias than the other TWs) applied to the three TW electrodes above an ion escalator to facilitate efficient ion transfer between levels. A diagram depicting the new ion escalator region is shown in Figure 1C, and Figure 1D shows examples of symmetric and asymmetric TWs as applied to the separation and escalator TW electrodes, respectively. The TW electrodes in pink show the TW electrodes above the ion escalator that are independent from the surrounding TW electrodes in green. Note that the rightmost TW electrode possessed the same phase TW (designated TW_{ii}) as the leftmost TW electrode, and the middle TW electrode possessed a 45 phase-shifted TW (designated TW_{ii+1}). It was also possible to apply TWs with different speeds to the ion escalator. Different from our previously published design,[15] we also removed all but one reverse TW electrode across the ion escalator orifice and replaced the area with a guard electrode.

Data Acquisition and Handling. IMS-MS spectra were collected using a custom data acquisition algorithm and viewed using the Pacific Northwest National Laboratory (PNNL) unified ion mobility format (.UIMF) viewer. Standalone IMS spectra were collected using an oscilloscope (DPO 5204B, Tektronix Inc., Beaverton, OR, USA). All data were exported as .csv files and imported into MATLAB (Mathworks, Natick, MA, USA) for data processing and plotting. Baseline corrections for standalone data were performed in Origin 2021b (OriginLab Corporation, Northampton, MA, USA).

RESULTS AND DISCUSSION

Optimization of Ion Escalator Geometries Using Ion Trajectory Simulations. Ion escalators allow ultralong path lengths (>40 m) to be established in SLIM without ion cycling and have enabled separations over wide mobility ranges with ultrahigh resolution (resolving power ∼560).[15] Although ion escalators yield high ion transmission efficiency for high mobility ions, some low mobility ions can be lost even when general ion surfing conditions are used (i.e., low speed, high amplitude TWs). We hypothesize that ion losses arise from the fact that ions must traverse a long distance in one TW period to be efficiently transferred through an ion escalator, lest they roll-over a TW and encounter deleterious effects, such as space-charge from incoming ions. This distance was ∼5.5 mm in previous multilevel SLIM modules (board spacings and thicknesses were 3.15 and 2.35 mm, respectively), which is 5.5× longer than a standard TW electrode. When designing the miniSLIM, ion trajectory simulations were used to explore how the traversal distance affects ion transmission efficiency through ion escalators.

The effects of SLIM board thickness and board spacing (i.e., ion escalator length) were evaluated independently. Geometry files (.GEM) were used to create eight different ion escalator workspaces: five different board spacings (2.55, 2.70, 2.85, 3.00, and 3.15 mm at 2.35 mm board thickness) and three different board thicknesses (1.65, 2.00, and 2.35 mm at 3.15 mm board spacing). The transmission efficiencies of the same negative Agilent tuning mixture ions (m/z 602, 1034, 1334, 1634, 1934, 2234, 2534, and 2834; 1000 ions per m/z) previously used to evaluate transmission efficiency were evaluated. Table S1 in the Supporting Information also provides the geometric and electronic simulation parameters for the previously developed multilevel SLIM system (as starting parameters) and the miniSLIM. Simulated ion transmission efficiency was defined as the number of ions traversing the ion escalator in one TW period divided by the total number of ions simulated.

Plots of ion transmission efficiency versus SLIM board spacing show that the transmission efficiencies of high mobility ions (e.g., m/z 602, 1034, and 1334) remain high regardless of board spacing (Figure 2A). However, the transmission efficiencies of moderate-to-low mobility ions (e.g., m/z 1634−2834) decrease when board spacings exceeded 2.55 mm, and transmission efficiencies were lowest when the largest board spacing was evaluated (i.e., 3.15 mm). This data indicates that ion transmission efficiencies through ion escalators are highest when board spacings are small. Similarly, high ion transmission efficiencies were obtained for all ions when smaller board thicknesses (e.g., 1.65 mm) were used compared to larger board thicknesses (e.g., 2.00 and 2.35 mm) (Figure 2B). The main takeaway from these simulations is that ion transmission efficiencies are best when small ion traversal distances (i.e., board spacings + board thicknesses) are used. Based on these simulations, we implemented board spacings and thicknesses of 2.80 and 1.65 mm, respectively, for the miniSLIM. This establishes a total ion traversal distance of 4.45 mm, which is 1.05 mm smaller than used in previous SLIM modules. We note that, while 2.55 mm board spacings yielded the highest simulated transmission efficiencies, we chose to use slightly larger board spacings because they provide room for more ions to traverse the SLIM than smaller board spacings. Another reason we used 2.80 mm board

https://doi.org/10.1021/acs.analchem.1c04700
Anal. Chem. XXXX, XXX, XXX−XXX

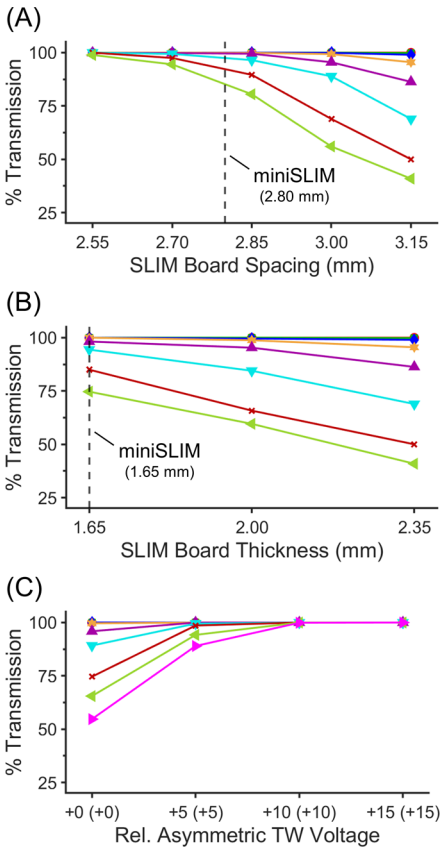

Figure 2. Simulated percent ion transmission efficiency plots of (−) Agilent tuning mixture ions traversing an ion escalator as a function of (A) SLIM board spacing and (B) SLIM board thickness using surfing traveling wave speeds. RF = 1 MHz, 300 V_{pp}, TW = 32 m/s, $15V_{0\text{-}p}$, guard = $-5V_{dc}$, P = 3.5 Torr He. Colors in panels (A, B) represent (−) AgTM ions with m/z (red) 602, (dark green) 1034, (blue) 1334, (orange) 1634, (purple) 1934, (light blue) 2234, (dark red) 2534, and (light green) 2834. (C) Simulated percent ion transmission efficiency plots of (+) Agilent tuning mixture ions traversing an ion escalator as a function of asymmetric TW bias (amplitude). RF = 1.5 MHz, 300 V_{pp}, TW = 24 m/s, $15V_{0\text{-}p}$, guard = $+5V_{dc}$, P = 2.5 Torr N_2. Colors in panel (C) represent (+) AgTM ions with m/z (red) 322, (dark green) 622, (blue) 922, (orange) 1222, (purple) 1522, (light blue) 1822, (dark red) 2122, (light green) 2422, and (pink) 2722.

spacings is to maximize the capturing of ions by the SLIM given that the conductance limiting orifice of the ion funnel trap preceding the miniSLIM has an i.d. of 2.50 mm. We also note that we utilized 1.65 mm board thickness for practical reasons (sturdiness and the multilayer construction of these double-sided PCBs).

A few notable advantages are apparent when using optimized SLIM board spacings and thicknesses. Ions possessing high and low mobilities can be efficiently transferred through the escalator in one TW period, which minimizes peak broadening and ion losses. However, what is more interesting is that better transmission efficiencies enable the use of nitrogen buffer gas for ion mobility separations. This is important because transmission efficiencies were only high when helium was used in previous multilevel SLIM systems. Nitrogen is more practical to use and better suited for miniature (and eventually portable) IMS systems, and the remainder of the data presented here (simulations and experiments) was collected using nitrogen.

Ion Transmission Efficiency Using Asymmetric TWs. After optimizing SLIM board spacings and thicknesses, a new method that uses asymmetric TWs to transfer ions between SLIM levels (instead of surfing TWs) was evaluated. We note that ion surfing happens when ions do not experience roll-over events during their movement with the TW and instead move at the same speed as the TWs. Ion surfing conditions can be achieved when the TW speed is sufficiently low (lower than ion velocity), or the TW amplitude is sufficiently high. The new method of transferring ions through the ion escalator involves applying asymmetric TWs to the three TW electrodes located directly above the ion escalator while keeping all other TW parameters the same (see Figure 1C,D). This idea was based on decreasing the complexity of using TWs with different speeds while maintaining similar or improved performance. Ion transmission efficiencies using different TW speeds (simulated and experimental) have been previously described.[15]

Ion trajectory simulations of positive AgTM ions (m/z 322, 622, 922, 1222, 1522, 1822, 2122, 2422, and 2722) were performed to explore how asymmetric TWs affect ion transmission efficiency through ion escalators. The buffer gas was 2.5 Torr nitrogen. Asymmetric TWs were established by adding a DC bias and providing larger TW amplitudes to the TWs applied to the three electrodes located directly above the ion escalator. We use the nomenclature $+V_{dc}$ ($+V_{0\text{-}p}$) to indicate relative increases in asymmetric TW voltages, and we note that these voltages are added on top of the already existing TW amplitude being applied to the other TW electrodes. For example, if a $15V_{0\text{-}p}$ TW is being applied to the separation TWs, then $+5V_{dc}$ ($+5V_{0\text{-}p}$) means that the asymmetric TW will possess a $+5V_{dc}$ bias and $20V_{0\text{-}p}$ TW amplitude. The asymmetric TW voltages were increased with a 1:1 ratio (e.g., $+5V_{dc}$ ($+5V_{0\text{-}p}$), $+10V_{dc}$ ($+10V_{0\text{-}p}$), etc.), which allowed us to obtain higher amplitude crests (i.e., tops of the square waves) while maintaining identical amplitude troughs (i.e., bottoms of the square waves). This was desired so that ions could be pushed through the ion escalator with more force than that of lower amplitude TWs.

Ion trajectory simulations using asymmetric TWs were performed, and plots of ion transmission efficiency versus relative asymmetric TW voltage show that asymmetric TWs work well to transfer ions between SLIM levels (Figure 2C). As can be seen, applying TWs with the same speed and amplitude as the surrounding TW electrodes (i.e., no asymmetric TW) results in ion losses, mostly associated with medium and low mobility ions (i.e., m/z 1522−2722). However, the transmission efficiencies greatly increase when a $+5V_{dc}$ ($+5V_{0\text{-}p}$) asymmetric TW is used, meaning that more ions are traversing the ion escalator in one TW period. Applying a $+10V_{dc}$ ($+10V_{0\text{-}p}$) asymmetric TW further increases transmission efficiencies to near 100%, and applying a $+15V_{dc}$ ($+15V_{0\text{-}p}$) achieves 100% transmission efficiency for all tested ions. Additionally, the transmission efficiencies of nine tetraalkylammonium cations were evaluated using the same asymmetric TW voltages. However, all TAA ions transferred through the ion escalators in one TW period under all conditions, which is attributed to their higher mobilities as compared to most AgTM ions.

Characterization of miniSLIM-MS Performance. The results of the ion trajectory simulations showed that small PCB spacings and PCB thicknesses should be used when employing ion escalators and that asymmetric TWs work well to transfer

https://doi.org/10.1021/acs.analchem.1c04700
Anal. Chem. XXXX, XXX, XXX−XXX

ions between levels. This knowledge was used to fabricate and assemble a multilevel miniSLIM platform that possessed three ion levels (two ion escalators) with a total path length of ~1 m. The main advantage of this miniSLIM is that the 1 m path length is established in a very compact format and without having to cycle ions, meaning that a wide mobility range can be analyzed. Initial experiments were performed by attaching the miniSLIM platform to TOF-MS and introducing the same positive AgTM ions examined in simulations using 3.5 Torr nitrogen buffer gas. Relative asymmetric voltages of $+20V_{dc}$ ($+20V_{0\text{-}p}$) were applied to the three ion escalator TW electrodes, and ions were injected using an IFT (488 μs injection time). Voltages, frequencies, and pressures were optimized to produce the highest signal intensities. A full characterization of asymmetric TW performance is provided later.

A mobility spectrum of AgTM cations was produced after summing 500 individual separations (Figure 3A, green trace).

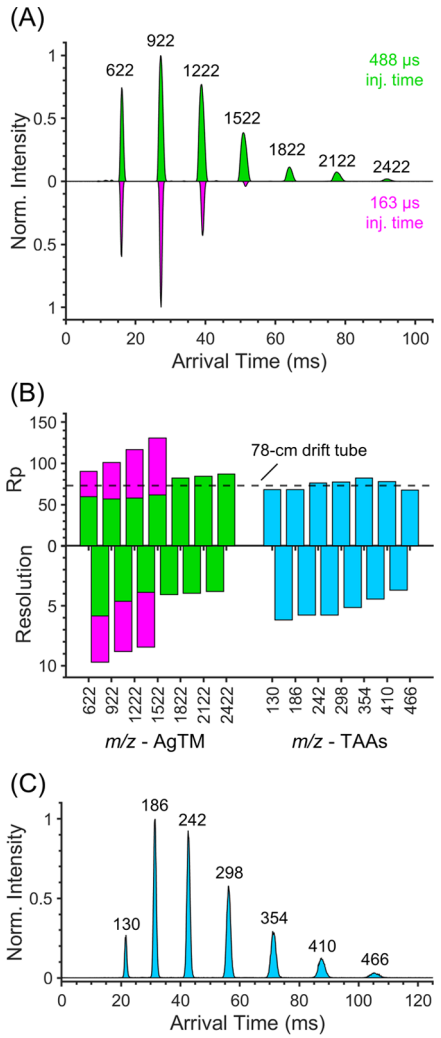

Figure 3. (A) IMS spectra of AgTM cations acquired using a multilevel miniSLIM module and injection times of (green) 488 and (pink) 163 μs. TW_{asym} = $+20V_{dc}$ ($+20V_{0\text{-}p}$). $Pressure_{SLIM}$ = 3.5 Torr nitrogen. (B) Resolving power and resolution calculations of AgTM and TAA cations. The dashed line indicates the highest resolving power obtained in ref 19 with a 78 cm drift tube. (C) IMS spectra of TAA cations. TW_{asym} = $+10V_{dc}$ ($+10V_{0\text{-}p}$). $Pressure_{SLIM}$ = 2.3 Torr nitrogen.

As can be seen, AgTM ions with m/z 622−2422 were readily observed and baseline-separated, which represents a clear separation of ions possessing widely varying mobilities with a miniature SLIM instrument. The data also represents the successful transfer of high and low mobility ions through two ion escalators in a nitrogen buffer gas. Collisional cross section-based resolving powers (R_p(CCS)) were calculated by converting the arrival times of the AgTM ions to the CCS domain using CCS values from Stow et al.[18] and applying eq 1

$$R_p(\mathrm{CCS}) = \frac{\mathrm{CCS}}{\Delta\mathrm{CCS}} \quad (1)$$

where CCS is taken at the peak center and ΔCCS is the full width at half-maximum (fwhm) of the peak in the CCS domain. The resolving powers of the high mobility AgTM ions (m/z 622, 922, 1222, and 1522) were between 58 and 62, while the low mobility AgTM ions (m/z 1822, 2122, and 2422) were between 83 and 87 (Figure 3B, green bars). The resolving powers obtained for the miniSLIM using 488 μs injection times were similar to the highest resolving power acquired by Ibrahim et al. using a 78 cm drift tube and singly charged ions, which was ~73.[19] These data represent the resolving powers and resolutions expected during routine analysis using a miniSLIM-MS module.

To determine the highest resolving power achievable using the miniSLIM, AgTM ions were injected using a 163 μs injection time at 3.5 Torr nitrogen and 500 individual separations were summed (Figure 3A, pink trace). As expected, peaks were thinner when lower injection times were used, although there was a notable absence of lower mobility AgTM ions (i.e., m/z 1822−2422), which is attributed to ion gating effects. Resolving powers of the four observed AgTM ions at 163 μs injection times ranged between 90 (m/z 622) and 131 (m/z 1522) with an average of 110 (Figure 3B, pink bars). These values demonstrate that the miniSLIM can produce resolving powers up to ~1.5× higher than a previously used 78 cm drift tube operating at a similar pressure but at a fraction of the total size. It may be possible to improve resolving powers by further reducing injection times, possibly by using the tristate ion shutter developed by Kirk et al., which showed that resolving powers of ~140 could be achieved when using 1 μs injection times in a 30 cm drift tube.[20,21] However, the drift tube used by Kirk et al. was operated at high electric field strength and 15 Torr, which was 4 to 5× higher pressure than used in the miniSLIM.

Peak−peak resolutions were also calculated according to eq 2 using both injection times[22,23]

$$\mathrm{Res}_{pp} = 1.18 \times \frac{\mathrm{td}_2 - \mathrm{td}_1}{\mathrm{fwhm}_2 + \mathrm{fwhm}_1} \quad (2)$$

where td_i is the center of the ion arrival time distribution (ATD) for ion i and fwhm is the full width at half-maximum of the ion ATD in the time domain. Resolutions ranged between 3.8 and 5.9 using 488 μs injection times and 8.5 and 9.7 using 163 μs injection times (Figure 3B, green and pink bars).

The miniSLIM was also tuned to transmit very high mobility ions, which required applying higher RF frequencies to the IFT and miniSLIM (1.5 MHz for both) and lower RF amplitude in the IFT (~50 V_{pp}). The pressure in the SLIM chamber was set to 2.3 Torr N_2 to achieve optimal signal intensities. A mixture of seven TAAs was introduced using a 488 μs injection time and relative asymmetric voltages of $+10V_{dc}$ ($+10V_{0\text{-}p}$) (Figure

https://doi.org/10.1021/acs.analchem.1c04700
Anal. Chem. XXXX, XXX, XXX−XXX

3C, blue trace). As can be seen, all seven TAA cations were observed and baseline-separated. Resolving powers of the TAAs ranged between 68 and 92 with an average of 74, and resolutions ranged between 3.7 and 6.2 with an average of 5.2 (Figure 3B, blue bars). CCS values for TAAs were obtained from Campuzano et al.[24] These values are again similar to the resolving powers and resolutions obtainable using 78 cm path length drift tubes and showcase the miniSLIM's ability to separate high mobility ions in a nitrogen buffer gas.

Experimental Characterization of Asymmetric TWs. The purpose of applying asymmetric TWs to the ion escalator is to ensure efficient ion transfer between SLIM levels. A systematic study of the effect of asymmetric TW on experimental ion transmission was performed by varying relative asymmetric TW voltages and monitoring the number and intensities of AgTM cations. Ions were injected with 488 μs injection times, and separation TWs possessed speeds and amplitudes of 128 m/s and 17.5$V_{0\text{-}p}$, respectively.

Experiments began by applying high relative asymmetric TW voltages (+20V_{dc} (+20$V_{0\text{-}p}$)) to the ion escalator and then decreasing by +5 (+5$V_{0\text{-}p}$) until separation TW voltages (+0V_{dc} (+0$V_{0\text{-}p}$)) were reached (Figure 4A). Note that the

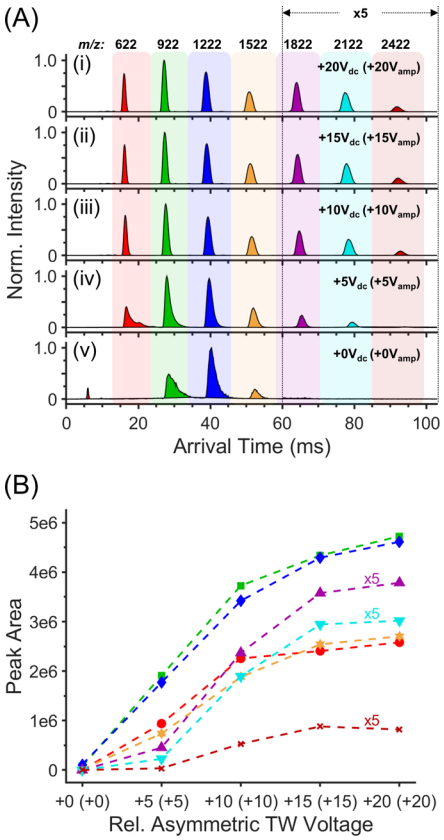

Figure 4. (A) IMS spectra and (B) extracted peak areas of AgTM cations as a function of asymmetric TW voltage (V_{dc} ($V_{0\text{-}p}$)).

mobility regions around m/z 1822, 2122, and 2422 (i.e., >60 ms) were multiplied five times to observe ion ATDs more easily. As can be seen, applying +20V_{dc} (+20$V_{0\text{-}p}$) resulted in the observation of seven AgTM cations, each with a relatively symmetric ATD (Figure 4A, inset (i)). Ion peak areas were extracted and plotted as a function of relative asymmetric TW voltage (Figure 4B) to better illustrate the effect of changing voltage. Decreasing the relative asymmetric TW voltage to +15V_{dc} (+15$V_{0\text{-}p}$) resulted in similar signal intensities for all ions compared to +20V_{dc} (+20$V_{0\text{-}p}$), which means that high asymmetric TW voltages do not appear to cause a high mobility cutoff (i.e., by giving high mobility ions enough momentum to crash into the electrodes on the bottom board). However, a noticeable drop in ion signal intensities was observed when decreasing to +10V_{dc} (+10$V_{0\text{-}p}$), indicating that some ions do not successfully traverse the ion escalators. Further decreasing to +5V_{dc} (+5$V_{0\text{-}p}$) results in the total loss of the lowest mobility ion (m/z 2422), lower signal intensities overall, and peak tailing for the three highest mobility ions (m/z 622, 922, and 1222). The tailing indicates that ions did not traverse the ion escalator in one TW period but were also not lost. Last, removing the relative asymmetric TW voltages shows a total loss of the low mobility ions and significant peak tailing for all other ions.

This data demonstrates that applying even a small asymmetric TW significantly improves ion transmission through ion escalators and that high asymmetric TWs successfully transmit ions without observable deleterious effects (over the voltage range used). Since one of the goals of implementing the asymmetric TWs was to be an alternative to the previous method of transferring ions between SLIM levels (i.e., using separation and surfing TWs), a set of comparison mobility spectra was acquired by keeping the speed of the TW applied to the separation region constant (i.e., 128 m/s, 17.5$V_{0\text{-}p}$) and varying the speed of the TW applied to the ion escalator region (e.g., 128, 64, 32, and 16 m/s). The ion escalator region includes the TW electrodes surrounding the ion transfer region (i.e., the orifice) and the electrodes inside the orifice. Schematics depicting separation and ion escalator TW electrodes and the speed of TWs applied to each region are given in the Supporting Information (Figure S2). The mobility spectra acquired by varying the speed of the ion escalator TW along with extracted peak areas are also shown in the Supporting Information (Figure S3). As can be seen, peak areas and ATD shapes generally improved as lower TW speeds were used in the ion escalator. However, high mobility ions can be slightly lost, especially when a low TW speed is used (i.e., 128:16 m/s). This means that the speed of the TW applied to the ion escalator must be tuned depending on the mobility range being transferred to avoid losses.

An experiment to compare the highest resolving powers and resolutions achievable using the asymmetric and TW speed ratio methods was performed using +20V_{dc} (+20$V_{0\text{-}p}$) and 128:16 m/s, respectively. Overlaid mobility spectra collected using AgTM cations and injection times of 163 μs at 3.5 Torr nitrogen using both methods and a plot of resolving power and resolution calculations are shown in the Supporting Information (Figure S4). The highest asymmetric TW voltage yielded approximately 10% (and up to 25%) higher resolving powers and resolutions than those obtained by applying a low TW speed to the ion escalator. We note however that both methods are viable ways to transfer ions between SLIM levels.

Experiments were also performed where combinations of asymmetric TWs and surfing TWs were used to evaluate if wider mobility ranges and more symmetric ATD shapes could be obtained. The mobility spectra of 12 combinations of asymmetric TWs (+0V_{dc} (+0$V_{0\text{-}p}$), +5V_{dc} (+5$V_{0\text{-}p}$), and +10V_{dc} (+10$V_{0\text{-}p}$)) and TW speed ratios (128:128, 128:64, 128:32, and 128:16 m/s) are shown in the Supporting Information (Figure S5). TAA cations were used for this study. As can be seen, there is little difference between when an asymmetric TW

https://doi.org/10.1021/acs.analchem.1c04700
Anal. Chem. XXXX, XXX, XXX−XXX

was combined with a TW speed ratio and when one was not. We rationalize that ions are moving under surfing conditions when a slow TW is being applied, and increasing the amplitude (and DC offset) of the surfing TW will not change this. We note that our power supply could not produce asymmetric TW voltages above +10V_{dc} (+10$V_{0\text{-}p}$) when combined with surfing TWs.

A final set of characterization experiments explored the effects of the asymmetric TW bias and amplitude independent from one another. Nine ion mobility spectra acquired using combinations of 0, 5, and 10V_{dc} and 0, 5, and 10$V_{0\text{-}p}$ are shown in the Supporting Information (Figure S6). The results indicate that applying a DC bias without an increased TW amplitude (i.e., +5V_{dc} (+0$V_{0\text{-}p}$) and +10V_{dc} (+0$V_{0\text{-}p}$)) improved ion ATD shapes and the transmitted mobility range. Alternatively, increasing the TW amplitude without a DC bias minimally improved spectral quality. However, the combination of DC bias and increased TW amplitude (equal values in particular) yielded mobility spectra with the most symmetric ion ATD shapes and widest mobility range, which agrees well with ion trajectory simulations.

Operation of miniSLIM as a Standalone System. A significant benefit of high performance miniature IMS systems is their ability to operate as standalone systems (i.e., IMS separations only). The performance of the miniSLIM as a standalone system was evaluated by detaching the miniSLIM from TOF-MS and using a charge sensing particle detector (CSPD) (see Figure 1A). A photograph of the standalone miniSLIM assembly is shown in Figure 5A.

The mobility spectra of AgTM ions were acquired using 488 μs injection times, and 450 individual separations were averaged using the standalone system (Figure 5B). Relative asymmetric TW voltages were +20V_{dc} (+20$V_{0\text{-}p}$). Baseline separation was again achieved, and the full mobility range of AgTM ions was observed, including the lowest mobility ion (m/z 2722). Sodiated adducts of several low mobility ions were also observed adjacent to the protonated species. We note that the IMS spectra collected using the CSPD required the application of a digital Fourier transform filter to remove interference from RF and TWs and also a baseline correction to account for CSPD response. The raw arrival time measurements and data processing workflow for AgTM cations are shown in the Supporting Information (Figure S7).

A preliminary demonstration of the miniSLIM's ability to separate biologically relevant compounds was performed by analyzing a mixture of nine standard peptides and averaging 500 individual separations (Figure 5C, red trace). For comparison, mobility spectra were obtained using the IMS-TOF-MS configuration (Figure 5C, blue trace) and a list of detected peptides with charge states and arrival times is provided in the Supporting Information (Table S2). Note that two sections of the IMS-MS spectra were zoomed in to observe small features more easily (72−130 ms = 10× and > 130 ms = 1000×). As can be seen, there is good correlation between the standalone IMS and IMS-MS spectra. Eight of the nine peptides were successfully detected in the IMS-MS spectra as either the 1+, 2+, 3+, or 4+ charge state with protonated and/or sodiated adducts. The smallest and largest ions detected (and able to be assigned) were 386.5 (kemptide^{2+}) and 1423 (melittin^{2+}), respectively. While standards would need to be analyzed to assign peaks in the standalone system, these IMS spectra establish a strong foundation for using multilevel SLIM technology to analyze biologically relevant mixtures over a wide mobility range without having to cycle ions to obtain high quality separations.

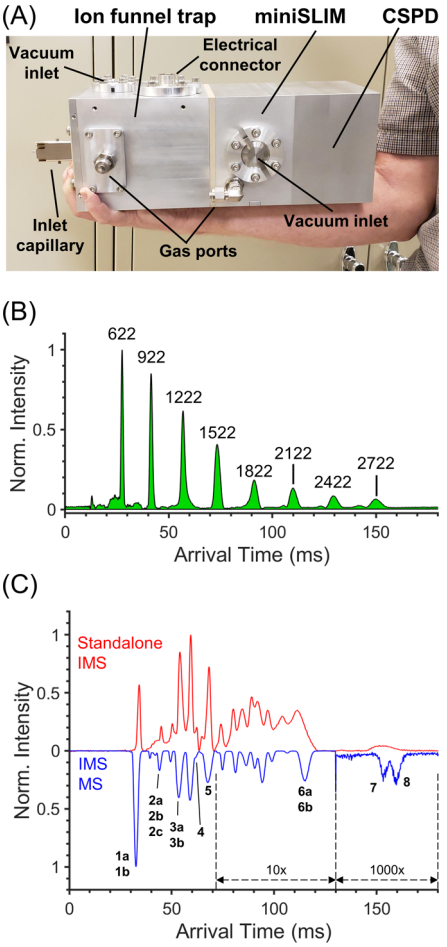

Figure 5. (A) Photograph of the standalone miniSLIM assembly. (B) IMS spectra of AgTM cations acquired using a standalone miniSLIM. TW_{sep} = 192 m/s, 15$V_{0\text{-}p}$. (C) IMS spectra of a mixture of nine standard peptides acquired using (red) a standalone miniSLIM and (blue) miniSLIM-TOF-MS. TW_{sep} = 192 m/s, 15$V_{0\text{-}p}$. $Pressure_{SLIM}$ = 3.5 Torr nitrogen.

CONCLUSIONS

We report the performance of a 1 m path length miniSLIM as a hybrid IMS-MS instrument and as a standalone system. We demonstrate a new method of transferring ions between SLIM levels using asymmetric TWs. Optimizing the ion escalator geometry and TW design facilitated high ion transmission efficiency for a wide range of ion mobilities and allowed nitrogen buffer gas to be used instead of helium. The miniSLIM yielded resolving powers of up to 1.5× higher than obtainable with a previously reported 78 cm drift tube for singly charged ions but at a fraction of the size.

A logical extension of this work could be to further increase the path length by adding SLIM levels while maintaining a similarly compact overall size. The present vacuum chamber can accommodate approximately nine levels (~3 m ion path length), which should provide a resolving power of ~220. Further improvements to ion transmission and ATD shapes are likely obtainable using higher relative asymmetric TW voltages. While the miniSLIM is quite small, it is not completely portable due to the current ancillary components,

https://doi.org/10.1021/acs.analchem.1c04700
Anal. Chem. XXXX, XXX, XXX−XXX

and improvements to make it so are underway, including miniaturizing and simplifying the power supplies, reducing the size of the ion detector housing, and implementing alternative ion injection and detection methods. For instance, the ion funnel trap can also be omitted and replaced by an ion trapping and accumulation region integrated into one of the miniSLIM levels. A Faraday detector can also help reduce the size and the need for baseline correction. Pulsed ion and gas introduction, as implemented by Cooks and co-workers,[25] as well as alternative ionization and ion introduction methods can be implemented to greatly reduce pumping requirements. Optimizing mobility separations for air as the buffer gas will also significantly enhance the attractiveness of the multilevel miniSLIM IMS system. Such large additional gains serve to make the miniSLIM IMS highly attractive for future standalone instrumentation.

■ ASSOCIATED CONTENT

Supporting Information

The Supporting Information is available free of charge at https://pubs.acs.org/doi/10.1021/acs.analchem.1c04700.

Geometric and electronic parameters of experimental miniSLIM, simulated original multilevel SLIM, and simulated miniSLIM systems; photographs of the miniSLIM analyzer; schematics of the ion escalator operating with TW speed ratios; ion mobility spectra and extracted peak areas of AgTM cations acquired using four different TW speed ratios; performance comparison of asymmetric TWs and TW speed ratios; ion mobility spectra of TAA cations obtained using a combination of asymmetric TWs and TW speed ratios; effects of independently varying the DC voltage and TW amplitude components of an asymmetric TW; data filtering and processing workflow for the standalone miniSLIM; and a list of detected peptides in a nine-peptide mixture using IMS-MS (PDF)

■ AUTHOR INFORMATION

Corresponding Author

Yehia M. Ibrahim − *Biological Sciences Division, Pacific Northwest National Laboratory, Richland, Washington 99354, United States;* orcid.org/0000-0001-6085-193X; Email: yehia.ibrahim@pnnl.gov

Authors

Adam L. Hollerbach − *Biological Sciences Division, Pacific Northwest National Laboratory, Richland, Washington 99354, United States*

Randolph V. Norheim − *Biological Sciences Division, Pacific Northwest National Laboratory, Richland, Washington 99354, United States*

Pearl Kwantwi-Barima − *Biological Sciences Division, Pacific Northwest National Laboratory, Richland, Washington 99354, United States*

Richard D. Smith − *Biological Sciences Division, Pacific Northwest National Laboratory, Richland, Washington 99354, United States;* orcid.org/0000-0002-2381-2349

Complete contact information is available at: https://pubs.acs.org/10.1021/acs.analchem.1c04700

Notes

The authors declare no competing financial interest.

■ ACKNOWLEDGMENTS

This work utilized capabilities developed under the support of the PNNL Laboratory Directed Research and Development (LDRD) and the National Institute of General Medical Sciences (R01 GM130709-01). This project was performed in the Environmental Molecular Sciences Laboratory, a DOE OBER national scientific user facility on the PNNL campus. PNNL is a multiprogram national laboratory operated by Battelle for the DOE under contract DE-AC05-76RL01830.

■ REFERENCES

(1) Ahrens, A.; Hitzemann, M.; Zimmermann, S. *Int. J. Ion Mobility Spectrom.* **2019**, *22*, 77−83.

(2) Bohrer, B. C.; Merenbloom, S. I.; Koeniger, S. L.; Hilderbrand, A. E.; Clemmer, D. E. *Annu. Rev. Anal. Chem.* **2008**, *1*, 293−327.

(3) Glaskin, R. S.; Ewing, M. A.; Clemmer, D. E. *Anal. Chem.* **2013**, *85*, 7003−7008.

(4) Cumeras, R.; Figueras, E.; Davis, C. E.; Baumbach, J. I.; Gràcia, I. *Analyst* **2015**, *140*, 1376−1390.

(5) Cumeras, R.; Figueras, E.; Davis, C. E.; Baumbach, J. I.; Gràcia, I. *Analyst* **2015**, *140*, 1391−1410.

(6) Fernandez-Lima, F.; Kaplan, D. A.; Suetering, J.; Park, M. A. *Int. J. Ion Mobility Spectrom.* **2011**, *14*, 93−98.

(7) Shvartsburg, A. A.; Clemmer, D. E.; Smith, R. D. *Anal. Chem.* **2010**, *82*, 8047−8051.

(8) Giles, K.; Ujma, J.; Wildgoose, J.; Pringle, S.; Richardson, K.; Langridge, D.; Green, M. *Anal. Chem.* **2019**, *91*, 8564−8573.

(9) Ben Faleh, A.; Warnke, S.; Rizzo, T. R. *Anal. Chem.* **2019**, *91*, 4876−4882.

(10) Bansal, P.; Yatsyna, V.; AbiKhodr, A. H.; Warnke, S.; Ben Faleh, A.; Yalovenko, N.; Wysocki, V. H.; Rizzo, T. R. *Anal. Chem.* **2020**, *92*, 9079−9085.

(11) Hamid, A. M.; Ibrahim, Y. M.; Garimella, S. V. B.; Webb, I. K.; Deng, L.; Chen, T.-C.; Anderson, G. A.; Prost, S. A.; Norheim, R. V.; Tolmachev, A. V.; Smith, R. D. *Anal. Chem.* **2015**, *87*, 11301−11308.

(12) Ibrahim, Y. M.; Hamid, A. M.; Deng, L.; Garimella, S. V. B.; Webb, I. K.; Baker, E. S.; Smith, R. D. *Analyst* **2017**, *142*, 1010−1021.

(13) Deng, L.; Ibrahim, Y. M.; Hamid, A. M.; Garimella, S. V. B.; Webb, I. K.; Zheng, X.; Prost, S. A.; Sandoval, J. A.; Norheim, R. V.; Anderson, G. A.; Tolmachev, A. V.; Baker, E. S.; Smith, R. D. *Anal. Chem.* **2016**, *88*, 8957−8964.

(14) Deng, L.; Webb, I. K.; Garimella, S. V. B.; Hamid, A. M.; Zheng, X.; Norheim, R. V.; Prost, S. A.; Anderson, G. A.; Sandoval, J. A.; Baker, E. S.; Ibrahim, Y. M.; Smith, R. D. *Anal. Chem.* **2017**, *89*, 4628−4634.

(15) Hollerbach, A. L.; Li, A.; Prabhakaran, A.; Nagy, G.; Harrilal, C. P.; Conant, C. R.; Norheim, R. V.; Schimelfenig, C. E.; Anderson, G. A.; Garimella, S. V. B.; Smith, R. D.; Ibrahim, Y. M. *Anal. Chem.* **2020**, *92*, 7972−7979.

(16) Ibrahim, Y. M.; Hamid, A. M.; Cox, J. T.; Garimella, S. V. B.; Smith, R. D. *Anal. Chem.* **2017**, *89*, 1972−1977.

(17) Ibrahim, Y.; Belov, M. E.; Tolmachev, A. V.; Prior, D. C.; Smith, R. D. *Anal. Chem.* **2007**, *79*, 7845−7852.

(18) Stow, S. M.; Causon, T. J.; Zheng, X.; Kurulugama, R. T.; Mairinger, T.; May, J. C.; Rennie, E. E.; Baker, E. S.; Smith, R. D.; McLean, J. A.; Hann, S.; Fjeldsted, J. C. *Anal. Chem.* **2017**, *89*, 9048−9055.

(19) Ibrahim, Y. M.; Baker, E. S.; Danielson, W. F., III; Norheim, R. V.; Prior, D. C.; Anderson, G. A.; Belov, M. E.; Smith, R. D. *Int. J. Mass Spectrom.* **2015**, *377*, 655−662.

(20) Kirk, A. T.; Grube, D.; Kobelt, T.; Wendt, C.; Zimmermann, S. *Anal. Chem.* **2018**, *90*, 5603−5611.

(21) Kirk, A. T.; Bohnhorst, A.; Raddatz, C.-R.; Allers, M.; Zimmermann, S. *Anal. Bioanal. Chem.* **2019**, *411*, 6229−6246.

(22) Dodds, J. N.; May, J. C.; McLean, J. A. *Anal. Chem.* **2017**, *89*, 12176−12184.

(23) Jeanne Dit Fouque, K.; Ramirez, C. E.; Lewis, R. L.; Koelmel, J. P.; Garrett, T. J.; Yost, R. A.; Fernandez-Lima, F. *Anal. Chem.* **2019**, *91*, 5021−5027.
(24) Campuzano, I.; Bush, M. F.; Robinson, C. V.; Beaumont, C.; Richardson, K.; Kim, H.; Kim, H. I. *Anal. Chem.* **2012**, *84*, 1026−1033.
(25) Gao, L.; Cooks, R. G.; Ouyang, Z. *Anal. Chem.* **2008**, *80*, 4026−4032.

https://doi.org/10.1021/acs.analchem.1c04700
Anal. Chem. XXXX, XXX, XXX−XXX